Circulating MicroRNA-122 Is Associated With The Risk of New-Onset Metabolic Syndrome And Type-2-Diabetes

Online Appendix

Northern blot. Hepatic miRNA-122 expression was assessed by Northern blot analysis as previously described (1). Briefly, total RNA (5μg) was separated on a 15% acrylamide TBE 8M urea gel and blotted onto a Hybond N+ nylon filter (Amersham Biosciences). DNA oligonucleotides complementary to mature miR-122 (5'- AAACACCATTGTCACACTCCA-3') were end-labeled with [α-^{32}P] ATP and T_4 polynucleotide kinase (New England Biolabs) to generate high-specific activity probes. Hybridization was carried out according to the ExpressHyb (Clontech) protocol. Following overnight membrane hybridization with specific radiolabeled probes, membranes were washed once for 30min at 42°C in 4x SSC/0.5% SDS and subjected to autoradiography. Blots were re-probed for 5S rRNA (5′-CAGGCCCGACCCTGCTTAGCTTCCGAGAGATCAGACGAGAT-3′) to control for equal loading.

Quantitative real-time PCR (qRT-PCR). Total RNA was isolated from liver and murine hepatocyte samples using the Bullet Blender Homogenizer (Next Advance) in TRIzol reagent (Invitrogen) according to the manufacturer's protocol. For mRNA quantification, cDNA was synthesized using iScript RT Supermix (Bio-Rad), following the manufacturer's protocol. qRT-PCR analysis was performed in triplicate using iQ SYBR green Supermix (BioRad) on an iCycler Real-Time Detection System (Eppendorf). The mRNA level was normalized to GAPDH or 18S as a house keeping gene (see primer sequence in Supplementary Table 5). For miRNA quantification, total RNA was reverse transcribed using the miScript II RT Kit

(Qiagen). Primers specific for mouse miR-122, miR-27b, miR148a and miR-33a (Qiagen) were used and values normalized to SNORD68 (Qiagen) (see Figure 2B). For gene expression analysis with qRT-PCR, total RNA was reversely transcribed using the high-capacity cDNA RT kit (Life Technologies). RT product (corresponding to 6.75 ng input RNA), 0.25µl Taqman gene expression assay (see Supplementary Table 6) and 2.5µl Taqman Universal PCR Master Mix No AmpErase UNG (2×) were combined in a total volume of 5µl. Cycling conditions were identical to miRNA analysis. GAPDH was used as a normalisation control.

Statin Treatment in Mice and Primary Murine Hepatocytes

Six week old, female C57Bl/6 mice were purchased from Harlan Laboratories (San Pietro al Natisone, Italy) and housed at 22°C under a 12h light/dark cycle under specific pathogen-free conditions with ad libitum access to chow and water. Mice were injected once a day with 20mg/kg atorvastatin intraperitoneally (Sigma Aldrich, Taufkirchen, Germany) for five days. Mice were sacrificed on day 5. Serum was collected by cardiac puncture. The liver was perfused with ice-cold phosphate-buffered saline and tissue specimens from the left lower lobe were either snap frozen or placed in RNAlater (Qiagen, Hilden, Germany) until further processing.

For *in vitro* experiments, primary mouse hepatocytes were isolated as previously described (2). Briefly, mice were anesthetized, the abdomen was opened and liver, vena cava, and portal vein were prepared. The liver was perfused regressively from the abdominal vena cava, via the liver veins (the vena cava proximal to the liver veins was occluded with a microclamp) to the portal vein using a peristaltic pump (Bio-Rad, Hercules, CA). The liver was first perfused using liver perfusion medium 1 supplemented with 0.1mM EGTA at a flow rate of 7 ml/min for 10min. Thereafter, liver perfusion medium 2 containing 30 µg/ml

Liberase TM (Roche, Mannheim, Germany) was used at a flow rate of 3.5 ml/min for another 10min. The liver was removed carefully and transferred into a petri-dish containing L-15 medium (Gibco, Carlsbad, CA). The capsule was incised and the resulting cell suspension was passed through a 100µm cell strainer. Hepatocytes were sedimented by low-speed centrifugation at 30 × g for 3min. Purity and viability were >90% after an isodensity Percoll centrifugation. 1.3×10^5 hepatocytes per cm^2 were seeded in William's E medium supplemented with 10% FCS and penicillin/streptomycin on collagen-coated 6-well plates. After resting cells overnight, hepatocytes were exposed to 0.1, 10, and 25 µM atorvastatin for 24h. Supernatants were harvested and cells were lysed in Buffer RLT. Both were stored at -80°C until further workup.

Plasma Proteomics in the Bruneck cohort

PlasmaDive kits (Biognosys AG) were used to profile plasma proteins in the Bruneck Study. Plasma samples were processed according to the manufacturer's instructions with one exception: peptide standards were spiked in before and not after tryptic digestion and C18 clean-up. Briefly, 10µl of plasma samples were denatured, reduced and alkylated. 20µg of proteins were spiked with 100 authentic heavy peptide standards. Seven proteins were below the limit of detection. An in-solution digestion was performed overnight. After solid phase extraction with C18 spin columns (96-well format, Harvard apparatus), the eluted peptides were dried using a SpeedVac (Thermo) and resuspended in 40µl of liquid chromatography (LC) solution. The samples were analysed on an Agilent 1290 LC system interfaced to an Agilent 6495 Triple Quadrupole MS. 10µl samples were directly injected onto a 25cm column (AdvanceBio Peptide Map 2.1 x 250mm) and separated over a 23min gradient at 300µl/min. The data were analysed using Skyline software version 3.1 (MacCross Lab) and protein concentrations were calculated using the heavy/light (H/L) ratio.

Proteomics of Liver Samples from AntagomiR-122 Treated Mice

Liver tissue was homogenized using Lysing Matrix D in radioimmunoprecipitation assay buffer (RIPA buffer) and protein concentrations were determined by the bicinchoninic acid assay (BCA). 20ug of protein from each liver sample were denatured with 6M urea/2M thiourea, reduced in 10mM DTT at 37 °C for 1h, and alkylated in 50mM iodoacetamide in the dark for 1h. Proteins were precipitated with ice cold acetone overnight and resuspended in 40 µl of 0.1M TEAB buffer, pH 8.2. Trypsin was added at a trypsin:protein ratio = 1:50 and proteins were digested overnight at 37 °C in agitation. The digestion was stopped by addition of 4 µl of 10% trifluoroacetic acid (TFA). Peptide samples were purified using C18 spin plate (Harvard Apparatus). The eluted peptides were dried using SpeedVac and resuspended in 40µl of 2% ACN + 0.05% TFA resulting in a final peptide-concentration of 0.5 µg/µl.

One microgram of digested peptides was separated using nano-flow HPLC (U3000 RSLCnano, C18 column, 75um ID x 50cm, Thermo Fisher Scientific) with the following gradient: 0-10min, 4%-10% B; 10-75min, 10%-30% B; 75-80min, 30%-40% B; 80-85min, 40%-99% B; 85-90min, 99% B; 90-120min, 4% B; where A=0.1% FA and B=80% ACN, 0.1% FA. The spectra were collected on a Q Exactive HF mass spectrometer (Thermo Fisher Scientific) with full MS scan range 350-1600 m/z (resolution 60,000) and top 15 most abundant precursor ions were selected for MS/MS in Orbitrap (resolution 15,000) with dynamic exclusion enabled. The data were searched against Uniprot mouse database (downloaded from ProteinCenter, version 2015-11-11, 24875 entries) using Proteome Discoverer 2.1 with Sequest HT. The following parameters were used: precursor mass tolerance=10ppm, fragment mass tolerance=0.02Da, trypsin as digestion enzyme and 2 missed cleavages allowed, carbamidomethylation of cysteines was used as fixed modification, oxidation of methionine as variable modification. The search results were loaded into Scaffold (version 4.3.2) and total TIC of each protein was used for quantification.

For TMT labelling, 10µg of peptide digests were concentrated using a SpeedVac and re-suspended at 1µg/µl using 10µl of 50mM TEAB. TMT labelling was carried out according to the manufacturer's instruction (TMT 10plex kit, QK226224, Thermo Fisher Scientific). After labelling, 10 samples were pooled together and dried down. The combined sample, containing a total of 100µg of peptide was then re-suspended in 100µl of 2% ACN + 0.05% TFA (1µg/µl). 1µg of mixed peptides was separated using nano-flow HPLC (U3000 RSLCnano, EASY-SPRAY C18 LC column, 75um ID x 50cm, Thermo Fisher Scientific) with the following gradient: 0-3min, 4% B; 3-10min, 4%-8%B; 10-200min, 8%-30% B; 200-210min, 30%-40% B; 210-215min, 40%-99%B; 215-220%, 99% B; 220-250min, 4% B; where A=0.1% FA and B=80% ACN, 0.1% FA.

The Synchronous Precursor Selection (SPS)-MS3 method was used on an Orbitrap Fusion Lumos Tribrid mass spectrometer (Thermo Fisher): Full MS on Orbitrap, scan range 375-1500 m/z (resolution 120,000), followed by data-dependant MS2 using CID fragmentation in ion trap using top speed mode with dynamic exclusion enabled, and synchronized precursor selection (SPS)-MS3 on the top 5 ions from the MS2 spectra in Orbitrap scan range 100-500 m/z (resolution 60,000) for the reporter ion using HCD fragmentation. The data were analysed using Proteome Discoverer 2.1. Sequest HT search was performed against UniProt mouse database (downloaded from ProteinCenter, version 2015-11-11, 24875 entries) with the following parameters: precursor mass tolerance=10ppm, fragment mass tolerance=0.6Da, trypsin as digestion enzyme and 2 missed cleavages allowed, carbamidomethylation of cysteines, TMT6plex on N-terminals and lysines, were used as fixed modification, oxidation of methionine as variable modification. The S/N of reporter ions from MS3 spectra were used for quantification with normalization and scaling option enabled.

References

1. Suárez Y, Fernández-Hernando C, Pober JS, Sessa WC. Dicer dependent microRNAs regulate gene expression and functions in human endothelial cells. Circ Res 2007;100:1164–1173.
2. Moschen AR, Gerner R, Schroll A, Fritz T, Kaser A, Tilg H. A key role for Pre-B cell colony-enhancing factor in experimental hepatitis. Hepatology 2011;54:675–686.
3. Fong MY, Zhou W, Liu L, et al. Breast-cancer-secreted miR-122 reprograms glucose metabolism in premetastatic niche to promote metastasis. Nat Cell Biol 2015;17:183–194.
4. Kojima S, Gatfield D, Esau CC, Green CB. MicroRNA-122 modulates the rhythmic expression profile of the circadian deadenylase Nocturnin in mouse liver. PLoS One 2010;5:e11264.
5. Tsai WC, Hsu SD, Hsu CS, et al. MicroRNA-122 plays a critical role in liver homeostasis and hepatocarcinogenesis. J Clin Invest 2012;122:2884–2897.
6. Iliopoulos D, Drosatos K, Hiyama Y, Goldberg IJ, Zannis VI. MicroRNA-370 controls the expression of microRNA-122 and Cpt1alpha and affects lipid metabolism. J Lipid Res 2010;51:1513–1523.
7. Liu T, Huang Y, Liu J, et al. MicroRNA-122 influences the development of sperm abnormalities from human induced pluripotent stem cells by regulating TNP2 expression. Stem Cells Dev 2013;22:1839–1850.
8. Kojima K, Takata A, Vadnais C, et al. MicroRNA122 is a key regulator of α-fetoprotein expression and influences the aggressiveness of hepatocellular carcinoma. Nat Commun 2011;2:338.
9. Davoodian N, Lotfi AS, Soleimani M, Mowla SJ. MicroRNA-122 overexpression promotes hepatic differentiation of human adipose tissue-derived stem cells. J Cell Biochem 2014;115:1582–1593.
10. Tanimizu N, Kobayashi S, Ichinohe N, Mitaka T. Downregulation of miR122 by grainyhead-like 2 restricts the hepatocytic differentiation potential of adult liver progenitor cells. Development 2014;141:4448–4456.

Supplementary Table 1 – Effect of antagomiR-122 injection on the hepatic proteome assessed using label-free proteomics. Proteins with P<0.05 are listed. Proteins that were also identified using proteomics with TMT-labelling are shown in **bold**.

Protein name	Accession Number	UniProt ID	Total TIC		Standardised mean difference	P value (unpaired t-test)
			Ctrl-miR (x10^6)	Anti-miR122 (x10^6)		
Nascent polypeptide-associated complex subunit alpha	Q60817	NACA_MOUSE	85±31	186±32	1.66	0.0009
Nascent polypeptide-associated complex subunit alpha, muscle-specific form	P70670	NACAM_MOUSE (+1)	85±31	186±32	1.66	0.0009
Dolichol-phosphate mannosyltransferase subunit 3	Q9D1Q4	DPM3_MOUSE	5±0	12±2	1.81	0.0015
Tropomyosin alpha-4 chain	Q6IRU2	TPM4_MOUSE	10±6	26±4	1.64	0.0015
Glucokinase	P52792-1	HXK4_MOUSE	15±7	103±29	1.75	0.0017
Isoform 2 of Glucokinase	P52792-2	HXK4_MOUSE	15±7	103±29	1.75	0.0017
Major vault protein	Q9EQK5	MVP_MOUSE	82±20	134±17	1.61	0.0021
ATP synthase F(0) complex subunit B1, mitochondrial	Q9CQQ7	AT5F1_MOUSE	572±103	922±145	1.60	0.0029
Importin-7	Q9EPL8	IPO7_MOUSE	15±2	25±1	1.78	0.0033
60S ribosomal protein L10A	P53026	RL10A_MOUSE	228±67	380±35	1.61	0.0040
NADH dehydrogenase [ubiquinone] iron-sulfur protein 2, mitochondrial	Q91WD5	NDUS2_MOUSE	150±23	94±22	-1.54	0.0046
Constitutive coactivator of PPAR-gamma-like protein 1	Q6A0A9	F120A_MOUSE	14±9	33±5	1.57	0.0047
Phenylalanine--tRNA ligase alpha subunit	Q8C0C7	SYFA_MOUSE	26±8	53±12	1.57	0.0047
Proteasome subunit beta type-8	P28063	PSB8_MOUSE	17±4	36±7	1.67	0.0052
Apolipoprotein B-100	E9Q414	APOB_MOUSE	14±10	35±6	1.54	0.0058
Isoleucine--tRNA ligase, cytoplasmic	Q8BU30	SYIC_MOUSE	27±6	14±5	-1.52	0.0058
Carnitine O-palmitoyltransferase 1, liver isoform	**P97742**	**CPT1A_MOUSE**	**164±42**	**254±36**	**1.50**	**0.0066**
Prosaposin	Q61207	SAP_MOUSE	808±163	1408±301	1.54	0.0074
V-type proton ATPase subunit G 1	Q9CR51	VATG1_MOUSE	39±9	59±9	1.47	0.0088
Carbonic anhydrase 2	P00920	CAH2_MOUSE	176±42	93±32	-1.48	0.0088
Guanine nucleotide-binding protein subunit beta-2-like 1	P68040	GBLP_MOUSE	524±69	672±68	1.46	0.0092
Ras GTPase-activating protein-binding protein 1	P97855	G3BP1_MOUSE	26±8	42±6	1.47	0.0095
Solute carrier family 22 member 1	O08966	S22A1_MOUSE	25±5	34±4	1.45	0.0098
Tubulin beta-5 chain	P99024	TBB5_MOUSE	55±47	142±29	1.48	0.0101
Haloacid dehalogenase-like hydrolase domain-containing protein 3	Q9CYW4	HDHD3_MOUSE	49±26	97±12	1.52	0.0104
Isoform 3 of Sec1 family domain-containing protein 1	Q8BRF7-3	SCFD1_MOUSE	8±2	14±3	1.54	0.0111
NADPH:adrenodoxin oxidoreductase, mitochondrial	Q61578	ADRO_MOUSE	35±9	13±8	-1.55	0.0111
Sec1 family domain-containing protein 1	Q8BRF7	SCFD1_MOUSE	8±2	14±3	1.54	0.0111
Isoform 2 of Leukemia inhibitory factor receptor	P42703-2	LIFR_MOUSE	94±23	350±28	1.71	0.0115
Leukemia inhibitory factor receptor	P42703-1	LIFR_MOUSE	94±23	350±28	1.71	0.0115

Supplementary Table 1 (cont'd)

Protein name	Accession Number	UniProt ID	Total TIC		Standardised mean difference	P value (unpaired t-test)
			Ctrl-miR (x10^6)	Anti-miR122 (x10^6)		
Dynein light chain 2, cytoplasmic	Q9D0M5	DYL2_MOUSE	69±58	174±37	1.46	0.0117
L-lactate dehydrogenase C chain	P00342	LDHC_MOUSE	2680±228	3250±252	1.52	0.0118
Mitochondrial pyruvate carrier 2	Q9D023	MPC2_MOUSE	326±23	157±90	-1.56	0.0118
ATP-dependent RNA helicase DDX1	Q91VR5	DDX1_MOUSE	16±12	39±3	1.56	0.0122
Prolow-density lipoprotein receptor-related protein 1	**Q91ZX7**	**LRP1_MOUSE**	**15±3**	**58±22**	**1.57**	**0.0124**
40S ribosomal protein S16	**P14131**	**RS16_MOUSE**	**258±75**	**446±104**	**1.44**	**0.0128**
Putative L-aspartate dehydrogenase	Q9DCQ2	ASPD_MOUSE	298±29	206±52	-1.47	0.0129
Isoform 2 of Polyadenylate-binding protein 2	Q8CCS6-2	PABP2_MOUSE	10±1	4±2	-1.67	0.0134
Polyadenylate-binding protein 2	Q8CCS6	PABP2_MOUSE	10±1	4±2	-1.67	0.0134
28S ribosomal protein S31, mitochondrial	Q61733	RT31_MOUSE	37±4	23±3	-1.67	0.0134
Lysozyme c-2	P08905	LYZ2_MOUSE	5±1	13±1	1.71	0.0135
Lysozyme c-1	P17897	LYZ1_MOUSE	5±1	13±1	1.71	0.0135
GDH/6PGL endoplasmic bifunctional protein	Q8CFX1	G6PE_MOUSE	83±20	123±20	1.41	0.0135
S-methyl-5'-thioadenosine phosphorylase	Q9CQ65	MTAP_MOUSE	11±4	30±8	1.65	0.0137
Profilin-1	P62962	PROF1_MOUSE	302±114	510±101	1.39	0.0161
Endoplasmin	P08113	ENPL_MOUSE	1062±226	1500±235	1.38	0.0170
40S RIBOSOMAL PROTEIN S6	P62754	RS6_MOUSE	364±33	558±115	1.50	0.0173
Peptidyl-prolyl cis-trans isomerase FKBP5	Q64378	FKBP5_MOUSE	6±1	14±5	1.44	0.0174
Lactoylglutathione lyase	Q9CPU0	LGUL_MOUSE	764±120	1140±230	1.43	0.0176
Ran-specific GTPase-activating protein	P34022	RANG_MOUSE	25±8	38±4	1.43	0.0177
Isoform HSP105-beta of Heat shock protein 105 kDa	Q61699-2	HS105_MOUSE	17±7	30±7	1.38	0.0178
Heat shock protein 105 kDa	Q61699	HS105_MOUSE	17±7	30±7	1.38	0.0178
Isoform 2 of 1-phosphatidylinositol 4,5-bisphosphate phosphodiesterase eta-1	Q4KWH5-2	PLCH1_MOUSE	87±64	194±45	1.39	0.0179
Isoform 3 of 1-phosphatidylinositol 4,5-bisphosphate phosphodiesterase eta-1	Q4KWH5-3	PLCH1_MOUSE	87±64	194±45	1.39	0.0179
Isoform 4 of 1-phosphatidylinositol 4,5-bisphosphate phosphodiesterase eta-1	Q4KWH5-4	PLCH1_MOUSE	87±64	194±45	1.39	0.0179
1-phosphatidylinositol 4,5-bisphosphate phosphodiesterase eta-1	Q4KWH5	PLCH1_MOUSE	87±64	194±45	1.39	0.0179
ADP/ATP translocase 1	P48962	ADT1_MOUSE	1700±412	2400±316	1.38	0.0181
Sodium/potassium-transporting ATPase subunit beta-1	P14094	AT1B1_MOUSE	46±29	93±17	1.41	0.0184
Regulator of microtubule dynamics protein 2	Q8BSE0	RMD2_MOUSE	14±3	39±16	1.44	0.0195
Isoform RRp2 of Ribosome-binding protein 1	Q99PL5-10	RRBP1_MOUSE	142±25	290±92	1.47	0.0204
Isoform RRp5.4 of Ribosome-binding protein 1	Q99PL5-9	RRBP1_MOUSE	142±25	290±92	1.47	0.0204
Protein LYRIC	Q80WJ7	LYRIC_MOUSE	9±3	21±8	1.40	0.0208

Supplementary Table 1 (cont'd)

Protein name	Accession Number	UniProt ID	Total TIC		Standardised mean difference	P value (unpaired t-test)
			Ctrl-miR (x10^6)	Anti-miR122 (x10^6)		
Cytoplasmic dynein 1 heavy chain 1	Q9JHU4	DYHC1_MOUSE	13±7	28±9	1.35	0.0225
La-related protein 1	Q6ZQ58-1	LARP1_MOUSE	49±7	30±10	-1.45	0.0228
Aldehyde dehydrogenase family 16 member A1	Q571I9	A16A1_MOUSE	45±25	89±25	1.33	0.0233
DnaJ homolog subfamily C member 10	Q9DC23	DJC10_MOUSE	20±5	46±9	1.65	0.0239
Mitochondrial 2-oxoglutarate/malate carrier protein	Q9CR62	M2OM_MOUSE	38±11	76±26	1.40	0.0253
60S ribosomal protein L37a	**P61514**	**RL37A_MOUSE**	**52±17**	**107±37**	**1.39**	**0.0254**
40S ribosomal protein S18	**P62270**	**RS18_MOUSE**	**420±112**	**602±96**	**1.32**	**0.0254**
Isoform RRp1.8 of Ribosome-binding protein 1	Q99PL5-11	RRBP1_MOUSE	152±24	290±92	1.43	0.0262
Isoform RRp0 of Ribosome-binding protein 1	Q99PL5-12	RRBP1_MOUSE	152±24	290±92	1.43	0.0262
Isoform RRp61 of Ribosome-binding protein 1	Q99PL5-2	RRBP1_MOUSE	184±31	308±84	1.40	0.0265
Isoform RRp47 of Ribosome-binding protein 1	Q99PL5-3	RRBP1_MOUSE	184±31	308±84	1.40	0.0265
Isoform RRp41 of Ribosome-binding protein 1	Q99PL5-4	RRBP1_MOUSE	184±31	308±84	1.40	0.0265
Isoform RRp16.8 of Ribosome-binding protein 1	Q99PL5-5	RRBP1_MOUSE	184±31	308±84	1.40	0.0265
Isoform RRp15a of Ribosome-binding protein 1	Q99PL5-6	RRBP1_MOUSE	184±31	308±84	1.40	0.0265
Isoform RRp15b of Ribosome-binding protein 1	Q99PL5-7	RRBP1_MOUSE	184±31	308±84	1.40	0.0265
Isoform RRp10 of Ribosome-binding protein 1	Q99PL5-8	RRBP1_MOUSE	184±31	308±84	1.40	0.0265
Mitochondrial coenzyme A transporter SLC25A42	Q8R0Y8	S2542_MOUSE	6±2	18±8	1.37	0.0267
Aldehyde dehydrogenase, dimeric NADP-preferring	P47739	AL3A1_MOUSE	46±16	144±67	1.37	0.0269
Cytochrome P450 2A12	**P56593**	**CP2AC_MOUSE**	**198±51**	**348±103**	**1.37**	**0.0271**
Isoform 3 of APOBEC1 complementation factor	Q5YD48-3	A1CF_MOUSE	7±1	11±3	1.36	0.0275
Eukaryotic translation initiation factor 3 subunit D	O70194	EIF3D_MOUSE	9±2	22±8	1.43	0.0276
bone marrow stromal antigen 2	Q8R2Q8	BST2_MOUSE	10±2	6±2	-1.53	0.0277
Pyridoxal kinase	Q8K183	PDXK_MOUSE	122±32	73±25	-1.31	0.0278
Tetratricopeptide repeat protein 39C	Q8VE09	TT39C_MOUSE	29±21	66±16	1.42	0.0293
Phosphate carrier protein, mitochondrial	Q8VEM8	MPCP_MOUSE	420±277	824±52	1.42	0.0298
Ras-related protein Rab-8B	P61028	RAB8B_MOUSE	22±6	10±5	-1.43	0.0301
Isoform Alpha of LIM domain and actin-binding protein 1	Q9ERG0-2	LIMA1_MOUSE	16±5	34±13	1.37	0.0305
ADP-dependent glucokinase	Q8VDL4	ADPGK_MOUSE	9±1	5±1	-1.70	0.0307
Isoform 3 of ADP-dependent glucokinase	Q8VDL4-3	ADPGK_MOUSE	9±1	5±1	-1.70	0.0307
60S ribosomal protein L13a	P19253	RL13A_MOUSE	157±115	390±158	1.30	0.0309
Clathrin light chain A	O08585	CLCA_MOUSE	18±9	34±10	1.29	0.0311
Nicotinamide phosphoribosyltransferase	Q99KQ4	NAMPT_MOUSE	32±10	46±6	1.31	0.0315

Supplementary Table 1 (cont'd)

Protein name	Accession Number	UniProt ID	Total TIC		Standardised mean difference	P value (unpaired t-test)
			Ctrl-miR (x10^6)	Anti-miR122 (x10^6)		
Isocitrate dehydrogenase [NADP], mitochondrial	P54071	IDHP_MOUSE	514±58	616±66	1.28	0.0321
Isoform 2 of Peroxisomal acyl-coenzyme A oxidase 1	Q9R0H0-2	ACOX1_MOUSE	102±69	3±3	-1.33	0.0323
14 kDa phosphohistidine phosphatase	Q9DAK9	PHP14_MOUSE	24±16	61±19	1.46	0.0329
40S ribosomal protein S28	P62858	RS28_MOUSE	290±55	374±48	1.28	0.0329
60S ribosomal protein L10-like	P86048	RL10L_MOUSE	412±147	616±76	1.32	0.0332
Isoform 2 of Protein FAM63A	Q76LS9-2	FA63A_MOUSE	6±4	21±6	1.60	0.0336
Protein FAM63A	Q76LS9-1	FA63A_MOUSE	6±4	21±6	1.60	0.0336
Isoform 2 of Sulfotransferase family cytosolic 1B member 1	Q9QWG7-2	ST1B1_MOUSE	16±9	30±1	1.32	0.0340
Sulfotransferase family cytosolic 1B member 1	Q9QWG7-1	ST1B1_MOUSE	16±9	30±1	1.32	0.0340
60S ribosomal protein L23a	**P62751**	**RL23A_MOUSE**	**340±97**	**550±150**	**1.29**	**0.0348**
Medium-chain specific acyl-CoA dehydrogenase, mitochondrial	P45952	ACADM_MOUSE	502±100	640±57	1.30	0.0350
Cytochrome P450 2J5	O54749	CP2J5_MOUSE	20±7	35±10	1.29	0.0351
Isoform 2 of Clustered mitochondria protein homolog	Q5SW19-2	CLU_MOUSE	15±3	10±3	-1.27	0.0352
40S ribosomal protein S8	P62242	RS8_MOUSE	666±71	816±107	1.29	0.0354
Protein lin-7 homolog C	O88952	LIN7C_MOUSE	17±16	80±42	1.36	0.0356
Ras-related protein Rab-11B	P46638	RB11B_MOUSE	92±26	131±24	1.26	0.0360
serine/threonine-protein phosphatase PP1-alpha catalytic subunit	P62137	PP1A_MOUSE	10±3	35±18	1.35	0.0365
Glutathione S-transferase theta-2	Q61133	GSTT2_MOUSE	79±27	116±9	1.35	0.0368
40S ribosomal protein S11	P62281	RS11_MOUSE	318±35	472±114	1.35	0.0368
Acyl-coenzyme A thioesterase 13	Q9CQR4	ACO13_MOUSE	67±13	100±25	1.30	0.0376
Lysosome-associated membrane glycoprotein 1	P11438	LAMP1_MOUSE	89±27	137±30	1.31	0.0378
Transitional endoplasmic reticulum ATPase	Q01853	TERA_MOUSE	498±69	614±78	1.25	0.0380
Isoform 2 of AP-2 complex subunit beta	Q9DBG3-2	AP2B1_MOUSE	24±8	42±13	1.28	0.0385
AP-2 complex subunit beta	Q9DBG3	AP2B1_MOUSE	24±8	42±13	1.28	0.0385
Aromatic-L-amino-acid decarboxylase	O88533	DDC_MOUSE	119±49	184±24	1.30	0.0387
Peroxiredoxin-6	O08709	PRDX6_MOUSE	1440±230	1760±167	1.26	0.0388
Nucleoside diphosphate kinase 3	Q9WV85	NDK3_MOUSE	13±1	27±8	1.45	0.0392
40S ribosomal protein S13	P62301	RS13_MOUSE	398±85	526±79	1.25	0.0393
Mannose-1-phosphate guanyltransferase alpha	Q922H4	GMPPA_MOUSE	8±5	15±4	1.25	0.0394
N-acyl-aromatic-L-amino acid amidohydrolase (carboxylate-forming)	Q91XE4	ACY3_MOUSE	93±41	150±29	1.26	0.0396
Granulins	**P28798**	**GRN_MOUSE**	**73±52**	**142±28**	**1.29**	**0.0397**
Aldehyde oxidase 3	G3X982	AOXC_MOUSE	370±117	558±126	1.24	0.0403

Supplementary Table 1 (cont'd)

Protein name	Accession Number	UniProt ID	Total TIC		Standardised mean difference	P value (unpaired t-test)
			Ctrl-miR (x10^6)	Anti-miR122 (x10^6)		
Isoform Short of Heterogeneous nuclear ribonucleoprotein A1	P49312-2	ROA1_MOUSE	47±16	80±25	1.26	0.0420
proteasome subunit beta type-2	Q9R1P3	PSB2_MOUSE	44±22	73±12	1.27	0.0425
Isoform 2 of RNA-binding protein 14	Q8C2Q3-2	RBM14_MOUSE	9±2	6±1	-1.40	0.0426
RNA-binding protein 14	Q8C2Q3	RBM14_MOUSE	9±2	6±1	-1.40	0.0426
Isoform 2 of Galectin-9	O08573-2	LEG9_MOUSE	149±73	286±102	1.24	0.0427
Isoform 3 of Galectin-9	O08573-3	LEG9_MOUSE	149±73	286±102	1.24	0.0427
Galectin-9	O08573	LEG9_MOUSE	149±73	286±102	1.24	0.0427
UV excision repair protein RAD23 homolog B	P54728	RD23B_MOUSE	34±6	58±19	1.33	0.0427
60S ribosomal protein L7	P14148	RL7_MOUSE	504±61	622±89	1.24	0.0434
Isoform 3 of Microtubule-associated protein 4	P27546-3	MAP4_MOUSE	10±3	20±8	1.30	0.0435
Histidine triad nucleotide-binding protein 1	**P70349**	**HINT1_MOUSE**	**768±223**	**428±227**	**-1.23**	**0.0437**
Inorganic pyrophosphatase 2, mitochondrial	Q91VM9	IPYR2_MOUSE	29±11	61±15	1.55	0.0438
Glucose-6-phosphate 1-dehydrogenase X	Q00612	G6PD1_MOUSE	33±3	8±0	-1.72	0.0443
very long-chain acyl-CoA synthetase	O35488	S27A2_MOUSE	264±59	394±101	1.25	0.0443
Isoform 2 of Heterogeneous nuclear ribonucleoprotein A3	Q8BG05-2	ROA3_MOUSE	254±67	344±49	1.23	0.0444
Arylamine N-acetyltransferase 2	P50295	ARY2_MOUSE	5±2	8±1	1.31	0.0447
Cathepsin D	P18242	CATD_MOUSE	490±108	662±120	1.22	0.0448
Golgi reassembly-stacking protein 2	Q99JX3	GORS2_MOUSE	17±5	10±3	-1.37	0.0448
Ras-related protein Rab-11A	P62492	RB11A_MOUSE	92±26	130±25	1.22	0.0456
Myosin regulatory light chain 12B	Q3THE2	ML12B_MOUSE	98±48	158±15	1.27	0.0466
Ribonuclease inhibitor	Q91VI7	RINI_MOUSE	136±51	208±45	1.21	0.0469
UDP-glucuronosyltransferase 1-6	Q64435	UD16_MOUSE	69±65	170±71	1.21	0.0469
Peptidyl-tRNA hydrolase 2, mitochondrial	Q8R2Y8	PTH2_MOUSE	6±1	65±47	1.27	0.0470
Cathepsin B	P10605	CATB_MOUSE	368±140	560±116	1.22	0.0471
ATP-binding cassette sub-family B member 9	Q9JJ59-1	ABCB9_MOUSE	61±18	104±35	1.25	0.0485
Isoform 2 of ATP-binding cassette sub-family B member 9	Q9JJ59-2	ABCB9_MOUSE	61±18	104±35	1.25	0.0485
Gamma-butyrobetaine dioxygenase	Q924Y0	BODG_MOUSE	28±11	49±16	1.22	0.0485
Isoform 3 of Thioredoxin reductase 2, mitochondrial	Q9JLT4-3	TRXR2_MOUSE	30±8	18±7	-1.30	0.0492
NADPH--cytochrome P450 reductase	P37040	NCPR_MOUSE	252±27	292±28	1.20	0.0492
60S ribosomal protein L35	Q6ZWV7	RL35_MOUSE	226±38	364±113	1.28	0.0497

Supplementary Table 2 – Effect of antagomiR-122 injection on the hepatic proteome assessed using proteomics with TMT-labelling. Proteins with P<0.05 are listed. Proteins that were also identified using label-free proteomics are shown in **bold**.

Protein name	Accession Number	UniProt ID	Total TIC		Standardised mean difference	P value (unpaired t-test)
			Ctrl-miR (x10^6)	Anti-miR122 (x10^6)		
40S ribosomal protein S24	P16632-1	RS24_MOUSE	87.9±7.5	112.1±7.9	1.65	0.0011
Heterogeneous nuclear ribonucleoprotein L	Q8R081	HNRPL_MOUSE	113.0±9.2	87.0±6.7	-1.66	0.0012
40S ribosomal protein S29	P62274	RS29_MOUSE	89.8±8.4	110.2±6.4	1.59	0.0030
ATP synthase subunit delta, mitochondrial	Q9D3D9	ATPD_MOUSE	110.7±9.6	89.3±4.9	-1.60	0.0045
tRNA (Cytosine(34)-C(5))-methyltransferase	Q1HFZ0-1	NSUN2_MOUSE	114.3±13.1	85.7±8.9	-1.56	0.0049
Eukaryotic translation initiation factor 3 subunit L	Q8QZY1	EIF3L_MOUSE	88.7±5.6	111.3±10.7	1.57	0.0055
Ras GTPase-activating-like protein IQGAP2	Q3UQ44	IQGA2_MOUSE	92.3±6.5	107.7±6.7	1.51	0.0060
Protein-glutamine gamma-glutamyltransferase 2	P21981	TGM2_MOUSE	87.9±10.7	112.1±10.2	1.50	0.0065
Superoxide dismutase [Cu-Zn]	P08228	SODC_MOUSE	103.9±3.9	96.1±2.7	-1.51	0.0071
Serum albumin	P07724	ALBU_MOUSE	115.6±14.2	84.4±13.5	-1.49	0.0074
LIM and SH3 domain protein 1	Q61792	LASP1_MOUSE	92.8±2.6	107.2±7.0	1.58	0.0076
Actin-related protein 3	Q99JY9	ARP3_MOUSE	92.3±5.7	107.7±7.7	1.49	0.0078
Dipeptidyl peptidase 1	P97821	CATC_MOUSE	86.5±5.4	113.5±13.5	1.57	0.0081
Signal recognition particle receptor subunit alpha	Q9DBG7	SRPR_MOUSE	84.6±8.1	115.4±15.7	1.53	0.0082
Serine--tRNA ligase, cytoplasmic	P26638	SYSC_MOUSE	93.5±5.3	106.5±6.5	1.47	0.0093
Lupus La protein homolog	P32067	LA_MOUSE	92.3±5.4	107.7±8.2	1.48	0.0100
Coatomer subunit beta	Q9JIF7	COPB_MOUSE	93.3±6.5	106.7±6.5	1.43	0.0117
Myosin light polypeptide 6	Q60605	MYL6_MOUSE	91.3±6.4	108.7±9.6	1.46	0.0117
ATP synthase subunit g, mitochondrial	Q9CPQ8	ATP5L_MOUSE	103.6±3.4	96.4±3.8	-1.42	0.0133
Proteasome subunit beta type-3	Q9R1P1	PSB3_MOUSE	91.8±3.2	108.1±9.2	1.51	0.0137
60S ribosomal protein L37a	**P61514**	**RL37A_MOUSE**	**93.9±4.3**	**106.0±7.0**	**1.44**	**0.0144**
Glycerol kinase	Q64516-3	GLPK_MOUSE	93.1±6.1	106.9±7.8	1.41	0.0153
Mitochondrial glutamate carrier 1	Q9D6M3	GHC1_MOUSE	95.1±5.6	104.9±4.6	1.39	0.0164
Vigilin	Q8VDJ3	VIGLN_MOUSE	96.3±1.3	103.7±4.4	1.50	0.0168
40S ribosomal protein S18	**P62270**	**RS18_MOUSE**	**92.8±4.1**	**107.2±8.8**	**1.44**	**0.0177**
obg-like ATPase 1	Q9CZ30-1	OLA1_MOUSE	96.6±4.1	103.4±1.0	1.49	0.0191
Apolipoprotein A-I	Q00623	APOA1_MOUSE	115.8±19.6	84.3±7.2	-1.45	0.0194
Translocation protein SEC63 homolog	Q8VHE0	SEC63_MOUSE	84.6±18.6	115.4±13.6	1.38	0.0195
Estradiol 17-beta-dehydrogenase 2	P51658	DHB2_MOUSE	89.6±6.3	110.4±13.2	1.42	0.0198
Isoform LMW of Kininogen-1	O08677-2	KNG1_MOUSE	111.4±14.1	88.6±9.8	-1.37	0.0203

Supplementary Table 2 – (cont'd)

Protein name	Accession Number	UniProt ID	Total TIC		Standardised mean difference	P value (unpaired t-test)
			Ctrl-miR (x10^6)	Anti-miR122 (x10^6)		
40S ribosomal protein S16	**P14131**	**RS16_MOUSE**	**91.7±7.8**	**108.3±10.1**	**1.36**	**0.0207**
Signal recognition particle 9 kDa protein	P49962	SRP09_MOUSE	93.3±7.2	106.7±7.6	1.35	0.0209
Granulins	**P28798**	**GRN_MOUSE**	**88.0±11.7**	**111.9±14.5**	**1.35**	**0.0216**
Myosin-9	Q8VDD5	MYH9_MOUSE	91.8±9.2	108.2±9.0	1.35	0.0217
Mitochondrial ornithine transporter 1	Q9WVD5	ORNT1_MOUSE	88.1±10.0	111.9±15.4	1.36	0.0230
Protein transport protein Sec23A	Q01405	SC23A_MOUSE	93.8±7.7	106.2±6.0	1.34	0.0234
Carnitine O-palmitoyltransferase 1, liver isoform	**P97742**	**CPT1A_MOUSE**	**93.2±8.7**	**106.8±6.1**	**1.35**	**0.0235**
SEC14-like protein 4	Q8R0F9	S14L4_MOUSE	95.8±3.4	104.2±5.5	1.36	0.0244
ras-related protein Rab-7a	P51150	RAB7A_MOUSE	92.5±7.7	107.5±9.5	1.32	0.0259
60S ribosomal protein L10	Q6ZWV3	RL10_MOUSE	92.5±5.9	107.4±10.1	1.35	0.0268
Band 3 anion transport protein	P04919	B3AT_MOUSE	115.8±21.5	84.2±12.9	-1.34	0.0276
Beta-ureidopropionase	Q8VC97	BUP1_MOUSE	93.1±9.2	106.9±6.2	1.33	0.0277
CDGSH iron-sulfur domain-containing protein 3, mitochondrial	B1AR13	CISD3_MOUSE	90.6±9.8	109.4±12.0	1.31	0.0280
Ras-related protein Rab-35	Q6PHN9	RAB35_MOUSE	89.4±7.7	110.6±14.9	1.34	0.0297
60S ribosomal protein L11	Q9CXW4	RL11_MOUSE	95.2±3.7	104.8±6.8	1.33	0.0307
Monocarboxylate transporter 1	P53986	MOT1_MOUSE	84.1±8.8	116.0±23.1	1.36	0.0333
40S ribosomal protein S20	P60867	RS20_MOUSE	95.4±6.2	104.6±5.1	1.27	0.0344
Heme-binding protein 1	Q9R257	HEBP1_MOUSE	106.7±3.7	93.3±9.8	-1.35	0.0345
60S ribosomal protein L36a	P83882	RL36A_MOUSE	89.4±12.0	110.6±14.2	1.27	0.0346
Isoform 3 of Myosin-14	Q6URW6-3	MYH14_MOUSE	117.2±24.9	82.8±15.3	-1.29	0.0356
60S ribosomal protein L26	P61255	RL26_MOUSE	95.1±5.3	104.9±6.7	1.27	0.0357
26S proteasome non-ATPase regulatory subunit 3	P14685	PSMD3_MOUSE	94.8±7.3	105.2±5.3	1.28	0.0358
NADH dehydrogenase [ubiquinone] 1 alpha subcomplex subunit 2	Q9CQ75	NDUA2_MOUSE	106.0±8.6	94.0±6.0	-1.28	0.0359
Eukaryotic peptide chain release factor subunit 1	Q8BWY3	ERF1_MOUSE	110.5±13.2	89.5±13.3	-1.26	0.0365
Polypyrimidine tract-binding protein 1	P17225	PTBP1_MOUSE	93.0±9.3	107.0±8.3	1.26	0.0369
Malate dehydrogenase, cytoplasmic	P14152	MDHC_MOUSE	103.9±4.6	96.1±5.3	-1.26	0.0372
Tubulin alpha-1C chain	P68373	TBA1C_MOUSE	96.6±1.9	103.4±5.1	1.33	0.0372
peptidyl-prolyl cis-trans isomerase D	Q9CR16	PPID_MOUSE	95.1±6.5	104.9±6.0	1.25	0.0385
Clathrin heavy chain 1	Q68FD5	CLH1_MOUSE	97.7±3.1	102.3±2.9	1.25	0.0394
Thymosin beta-4	P20065	TYB4_MOUSE	83.0±6.4	117.0±25.7	1.35	0.0394
Cytosol aminopeptidase	Q9CPY7-1	AMPL_MOUSE	102.7±2.1	97.3±4.1	-1.29	0.0405
NADH dehydrogenase [ubiquinone] iron-sulfur protein 3, mitochondrial	Q9DCT2	NDUS3_MOUSE	106.9±5.0	93.1±10.6	-1.30	0.0406

Supplementary Table 2 – (cont'd)

Protein name	Accession Number	UniProt ID	Total TIC		Standardised mean difference	P value (unpaired t-test)
			Ctrl-miR (x10^6)	Anti-miR122 (x10^6)		
DNA damage-binding protein 1	Q3U1J4	DDB1_MOUSE	95.6±5.0	104.4±6.3	1.24	0.0411
Prolow-density lipoprotein receptor-related protein 1	**Q91ZX7**	**LRP1_MOUSE**	**95.2±6.6**	**104.8±5.9**	**1.24**	**0.0411**
Succinate dehydrogenase [ubiquinone] flavoprotein subunit, mitochondrial	Q8K2B3	SDHA_MOUSE	102.9±3.8	97.1±3.9	-1.24	0.0413
Fatty acid-binding protein 9	O08716	FABP9_MOUSE	84.9±16.3	115.1±22.0	1.24	0.0419
Integrin alpha-1	Q3V3R4	ITA1_MOUSE	91.2±11.4	108.8±11.6	1.23	0.0421
60S acidic ribosomal protein P1	P47955	RLA1_MOUSE	94.8±7.1	105.2±6.4	1.23	0.0426
5-hydroxyisourate hydrolase	Q9CRB3	HIUH_MOUSE	104.4±5.6	95.6±5.9	-1.23	0.0431
60S ribosomal protein L18	P35980	RL18_MOUSE	95.6±3.8	104.4±6.9	1.27	0.0435
Spliceosome RNA helicase DDX39B	Q9Z1N5	DX39B_MOUSE	94.1±6.8	105.9±8.5	1.23	0.0437
Plasminogen	P20918	PLMN_MOUSE	110.0±10.4	90.0±15.1	-1.24	0.0444
Fatty aldehyde dehydrogenase	P47740	AL3A2_MOUSE	94.5±6.1	105.5±8.2	1.23	0.0450
Succinate dehydrogenase [ubiquinone] iron-sulfur subunit, mitochondrial	Q9CQA3	SDHB_MOUSE	103.3±1.3	96.7±5.2	-1.32	0.0450
60S ribosomal protein L30	P62889	RL30_MOUSE	94.6±6.3	105.4±8.0	1.22	0.0454
Coatomer subunit alpha	Q8CIE6	COPA_MOUSE	94.6±3.0	105.5±8.7	1.30	0.0461
14-3-3 protein beta/alpha	Q9CQV8-1	1433B_MOUSE	96.8±2.5	103.2±5.1	1.26	0.0462
Histidine triad nucleotide-binding protein 1	**P70349**	**HINT1_MOUSE**	**105.7±7.9**	**94.4±7.4**	**-1.21**	**0.0475**
Alpha-1-antitrypsin 1-2	P22599	A1AT2_MOUSE	111.6±18.7	88.4±9.4	-1.25	0.0478
60S ribosomal protein L23a	**P62751**	**RL23A_MOUSE**	**92.3±7.5**	**107.7±12.2**	**1.23**	**0.0481**
Prostaglandin E synthase 3	Q9R0Q7	TEBP_MOUSE	95.4±2.7	104.6±7.4	1.28	0.0489
Cytochrome P450 2A12	**P56593**	**CP2AC_MOUSE**	**93.7±5.6**	**106.3±10.2**	**1.24**	**0.0490**
60S ribosomal protein L22	P67984	RL22_MOUSE	78.8±30.1	121.2±27.9	1.20	0.0495

Supplementary Table 3 – Predicted direct miR-122 targets and corresponding results from unlabelled and TMT-labelled proteomics.

Gene mouse (HUMAN)	Uniprot Name	Predicted mouse (x/12)	Predicted human (x/12)	Previously validated	Unlabelled proteomics	TMT-labelled proteomics
Pkm	KPYM_MOUSE	9	7	Luc Hs (3)	-	-
Aldh3a2	AL3A2_MOUSE	**6**	**5**	-	-	↑
Ccrn4l	NOCT_MOUSE	7	4	Luc Mm (4)	n.i.	n.i.
Fads1	FADS1_MOUSE	3	6	-	-	n.i.
Igf2	IGF2_MOUSE	6	3	Other Mm (5)	n.i.	n.i.
Myh9	MYH9_MOUSE	4	5	-	-	↑
Cpt1a	CPT1A_MOUSE	3	5	Other Mm (6)	↑	↑
Lgals3bp	LG3BP_MOUSE	5	3	Other Hs (7)	-	n.i.
Rab27a	RB27A_MOUSE	3	5	-	n.i.	n.i.
Tuba1c	TBA1C_MOUSE	1	7	-	-	↑
Eif3i	EIF3I_MOUSE	0	7	-	-	-
Lrp1	LRP1_MOUSE	3	4	-	↑	↑
Slc16a1	MOT1_MOUSE	5	1	-	-	↑
Slc25a15	ORNT1_MOUSE	2	4	-	-	↑
Auh	AUHM_MOUSE	4	1	-	-	-
Ldha	LDHA_MOUSE	4	1	-	-	-
Rpl23a	RL23A_MOUSE	1	4	-	↑	↑
Acsl1	ACSL1_MOUSE	2	2	-	n.i.	-
Apob	APOB_MOUSE	3	1	Other Hs (7)	↑	-
Vapa	VAPA_MOUSE	2	2	-	-	-
Iqgap2	IQGA2_MOUSE	1	2	-	-	↑
Afp	FETA_MOUSE	1	1	Other Hs (8), Other Mm (5)	n.i.	n.i.
Alb	ALBU_MOUSE	0	2	Other Hs (9), Other Mm (10)	-	↓
Apoa1	APOA1_MOUSE	1	1	-	-	↓
Asgr1	ASGR1_MOUSE	1	1	-	-	-
Grn	GRN_MOUSE	1	1	-	↑	↑
Hint1	HINT1_MOUSE	1	1	-	↓	↓
Rpl37a	RL37A_MOUSE	1	1	-	↑	↑
Cyp2a12 (CYP2A13)	CP2AC_MOUSE	0	1	-	↑	↑
Rps16	RS16_MOUSE	1	0	-	↑	↑
Rps18	RS18_MOUSE	0	0	-	↑	↑

Abbreviations: Other = Other miR-122 experiments in which the respective genes were regulated, not direct evidence for the gene being a target of miR-122; Luc = validation using luciferase assay; Hs = validation in human system or sequence; Mm = validation in mouse system or sequence; n.i. = not identified.

Supplementary Table 4 – MiRNAs in human HDL and VLDL.

	miRNA expression, C_t	
	VLDL particle	HDL particle
miR-24	28.8	32.0
miR-92a	31.8	35.8
miR-122	*Not detectable*	*Not detectable*
miR-126	30.0	29.1
miR-146a	30.9	36.1
miR-191	30.0	33.9
miR-223	23.5	24.8

MiRNAs were measured using RNA extracted from human HDL and VLDL samples. C_t, Cycle threshold.

Supplementary Table 5 – Primer sequences used to quantify expression of genes implicated in cholesterol and lipid metabolism at the mRNA level in antagomiR-122 treated mice, related to Fig. 2.

Gene	Forward (5'➔3')	Reverse (3'➔5')
18S	TTCCGATAACGAACGAGACTCT	TGGCTGAACGCCACTTGTC
Acc1	ATCCAGGCCATGTTGAGACG	AGATGTGCTGGGTCATGTGG
Acly	ATGCGAGTGCAGATCC	AAGGTAGTGCCCAATG
Aldo	TGAATAGGCTGCGTTCTCTTG	GCAGTGCTTTCCTTTCCTAACTC
Ampk	TGACCGGACATAAAGTGGCTGTGA	TGATGATGTGAGGGTGCCTGAACA
Cpt1	TTGATCAAGAAGTGCCGGACGAGT	GTCCATCATGGCCAGCACAAAGTT
Fasn	CTTCGCCAACTCTACCATGG	TTCCACACCCATGAGCGAGT
Gapdh	ACACATTGGGGGTAGGAACA	AACTTTGGCATTGTGGAAGG
Hmgcr	CTTGTGGAATGCCTTGTGATTG	AGCCGAAGCAGCACATGAT
Ldlr	GGTACTGGCAACCACCATTGGG	GCCAATCGACTCACGGGTTCAG
Mttp	AGGCAATTCGAGACAAAG	ACGTCAAAGCATATCGTTC
Scd1	CTGGAGATCTCTGGAGCATGTGGG	TACCCTTTGCTGGCAGCCGA
Srebp1	GCAGCCACCATCTAGCCTG	CAGCAGTGAGTCTCTGCCTTGAT
Srebp2	GCGTTCTGGAGACCATGGA	ACAAAGTTGCTCTGAAAACAAATCA

Supplementary Table 6 – Taqman assays used in Supplementary Fig. 3.

Gene	Taqman ID
Acsl1	Mm00484217_m1
Afm	Mm00446866_m1
Afp	Mm00431715_m1
Ahsg	Mm01145470_m1
Alb	Mm00802090_m1
Aldh3a2	Mm00839320_m1
Apoa1	Mm00437569_m1
Apob	Mm01545150_m1
Apoc2	Mm00437571_m1
Apoc3	Mm00445670_m1
Apoe	Mm01307193_g1
Asgr1	Mm01245581_m1
Auh	Mm00479363_m1
Azgp1	Mm00516331_m1
C3	Mm01232785_m1
Ccrn4l	Mm00802276_m1
Cebpa	Mm00514283_s1
Cfh	Mm01299248_m1
Cfi	Mm00432477_m1
Cpt1a	Mm01231183_m1
Crp	Mm00432680_g1
Ctsd	Mm00515586_m1
Cyp2a12	Mm00504878_m1
Eif3i	Mm00517000_m1
Fads1	Mm00507605_m1
Gapdh	Mm03302249_g1
Gpt	Mm00805379_g1
Grn	Mm00433848_m1
Hint1	Mm00801722_m1
Hp	Mm00516884_m1
Igf1	Mm00439560_m1
Igf2	Mm00439564_m1
Iqgap2	Mm01282618_m1
Ldha	Mm01612132_g1
Lgals3bp	Mm00478303_m1
Lox	Mm00495386_m1
Lrg1	Mm01278767_m1
Lrp1	Mm00464608_m1
Myh9	Mm01197036_m1
Pcsk9	Mm01263610_m1
Pkm	Mm00834102_gH
Rab27a	Mm00469997_m1
Rpl23a	Mm03020030_g1
Rpl37a	Mm01546394_s1
Rps16	Mm01617540_g1
Rps18	Mm02601777_g1
Slc16a1	Mm01306379_m1
Slc25a15	Mm01222280_m1
Sort1	Mm00490905_m1
Trib1	Mm00454875_m1
Tuba1c	Mm02528102_g1
Vapa	Mm00497141_m1
Vim	Mm01333430_m1
Vtn	Mm00495976_m1

Supplementary Figure 1 – Correlation of miR-122 over time and in serum vs. plasma in the Bruneck Study.

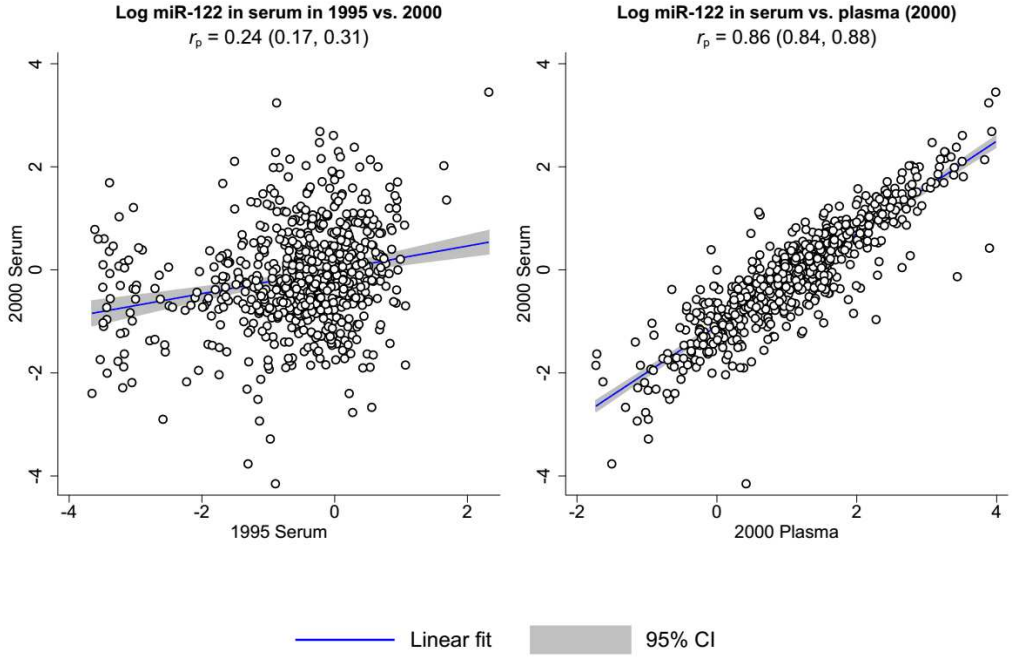

MiRNA values were log-transformed for analysis.

Supplementary Figure 2 – Correlation of serum miR-122 with circulating levels of proteins in the Bruneck Study.

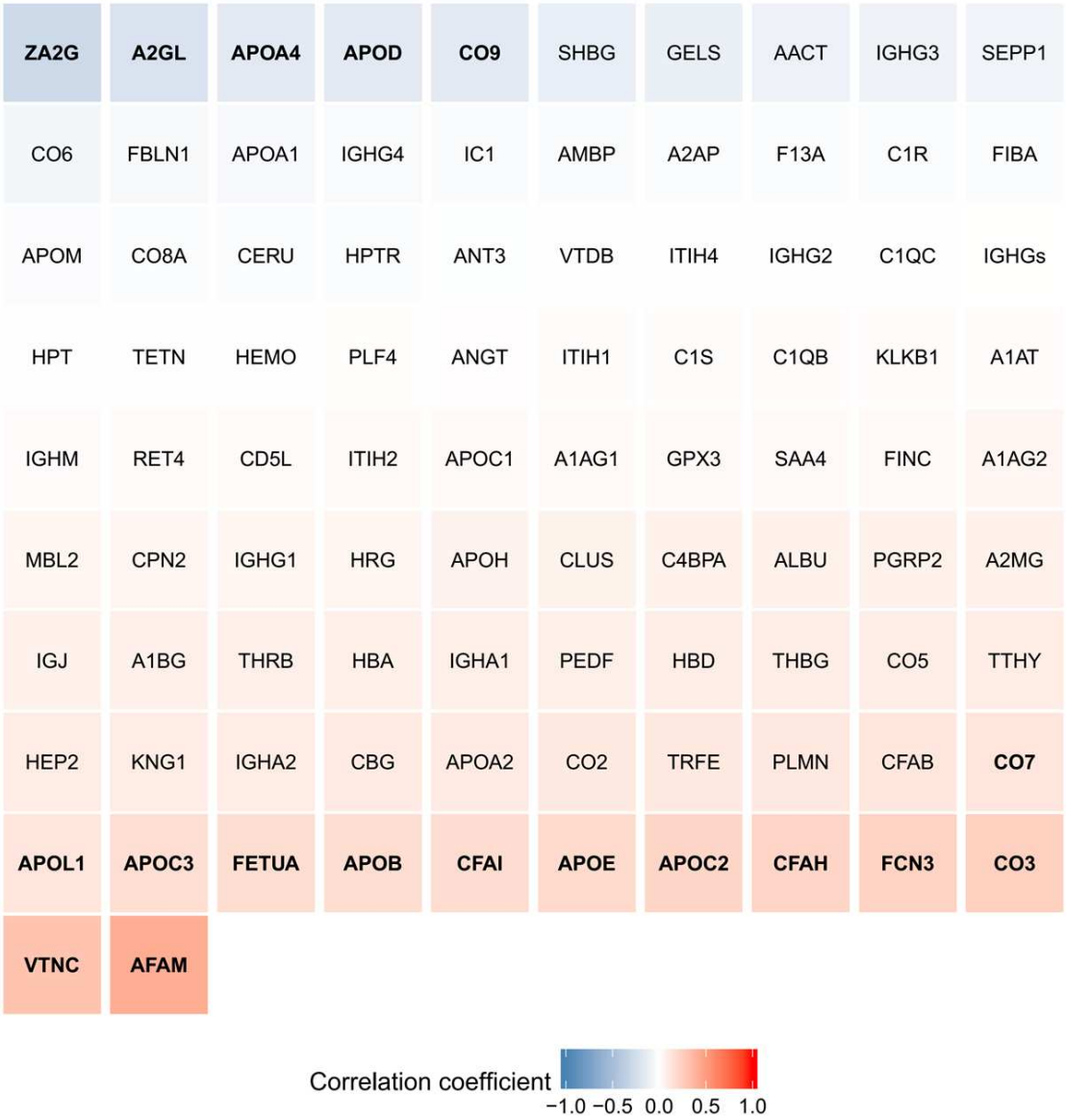

Spearman correlation coefficients were adjusted for age and sex. Proteins in bold were significant after Bonferroni-correction for multiple testing. Abbreviations: A1AG1, alpha-1-acid glycoprotein 1; A1AG2, alpha-1-acid glycoprotein 2; A1AT, alpha-1-antitrypsin; A1BG, alpha-1B-glycoprotein; A2AP, alpha-2-antiplasmin; A2GL, leucine-rich alpha-2-glycoprotein; A2MG, alpha-2-macroglobulin; AACT, alpha-1-antichymotrypsin; AFAM, afamin; ALBU, albumin; AMBP, alpha-1-microglobulin; ANGT, angiotensinogen; ANT3, antithrombin-III; APOA1, apolipoprotein A-I; APOA2, apolipoprotein A-II; APOA4, apolipoprotein A-IV; APOB, apolipoprotein B-100; APOC1, apolipoprotein C-I; APOC2, apolipoprotein C-II; APOC3, apolipoprotein C-III; APOD, apolipoprotein D; APOE, apolipoprotein E; APOH, apolipoprotein H; APOL1, apolipoprotein L1; APOM, apolipoprotein M; C1QB, complement C1q subcomponent subunit B; C1QC, complement

C1q subcomponent subunit C; C1R, complement C1r subcomponent; C1S, complement C1s subcomponent; C4BPA, C4b-binding protein alpha chain; CBG, corticosteroid-binding globulin; CD5L, CD5 antigen-like; CERU, ceruloplasmin; CFAB, complement factor B; CFAH, complement factor H; CFAI, complement factor I; CLUS, clusterin; CO2, complement C2; CO3, complement C3; CO5, complement C5; CO6, complement C6; CO7, complement C7; CO8A, complement C8 alpha chain; CO9, complement C9; CPN2, carboxypeptidase N subunit 2; F13A, coagulation factor XIII A chain; FBLN1, fibulin-1; FCN3, ficolin-3; FETUA, fetuin A; FIBA, fibrinogen alpha chain; FINC, fibronectin; GELS, gelsolin; GPX3, glutathione peroxidase 3; HBA, hemoglobin subunit alpha; HBD, hemoglobin subunit delta; HEMO, hemopexin; HEP2, heparin cofactor 2; HPT, haptoglobin; HPTR, haptoglobin-related protein; HRG, histidine-rich glycoprotein; IC1, plasma protease C1 inhibitor; IGHA1, immunoglobulin alpha 1; IGHA2, immunoglobulin alpha 2; IGHGs, immunoglobulin gamma; IGHG1, immunoglobulin gamma 1; IGHG2, immunoglobulin gamma 2; IGHG3, immunoglobulin gamma 3; IGHG4, immunoglobulin gamma 4; IGHM, immunoglobulin mu; IGJ, immunoglobulin J; ITIH1, inter-alpha-trypsin inhibitor heavy chain 1; ITIH2, inter-alpha-trypsin inhibitor heavy chain 2; ITIH4, inter-alpha-trypsin inhibitor heavy chain 4; KLKB1, kallikrein; KNG1, kininogen-1; MBL2, mannose-binding protein C; PEDF, pigment epithelium-derived factor; PGRP2, N-acetylmuramoyl-L-alanine amidase; PLF4, platelet factor 4; PLMN, plasminogen; RET4, retinol-binding protein 4; SAA4, serum amyloid A-4 protein; SEPP1, selenoprotein P; SHBG, sex hormone-binding globulin; TETN, tetranectin; THBG, thyroxine-binding globulin; THRB, prothrombin; TRFE, serotransferrin; TTHY, transthyretin; VTDB, vitamin D-binding protein; VTNC, vitronectin; ZA2G, zinc-alpha-2-glycoprotein.

Supplementary Figure 3 – (A) Volcano plots of all the qPCR data from antagomir-122 treated versus control liver samples, with the genes with P <0.05 highlighted in red. Details on the Taqman assay used is provided in Supplementary Table 6. (B) Detailed results for genes differentially expressed in the antagomiR-122 group vs. the control group, i.e. Alpha-fetoprotein, (Afp), IQ motif containing GTPase activating protein 2 (Iqgap2), and Ras-related protein (Rab27).

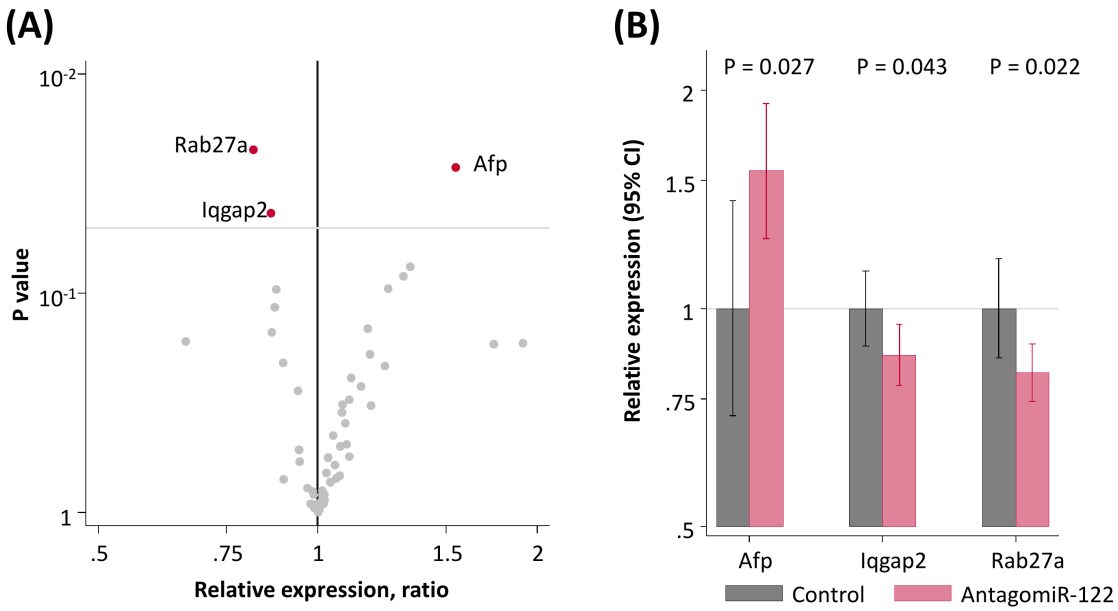

Supplementary Figure 4 – Association of miR-122 with metabolic syndrome and type-2 diabetes across clinically relevant subgroups in the Bruneck Study.

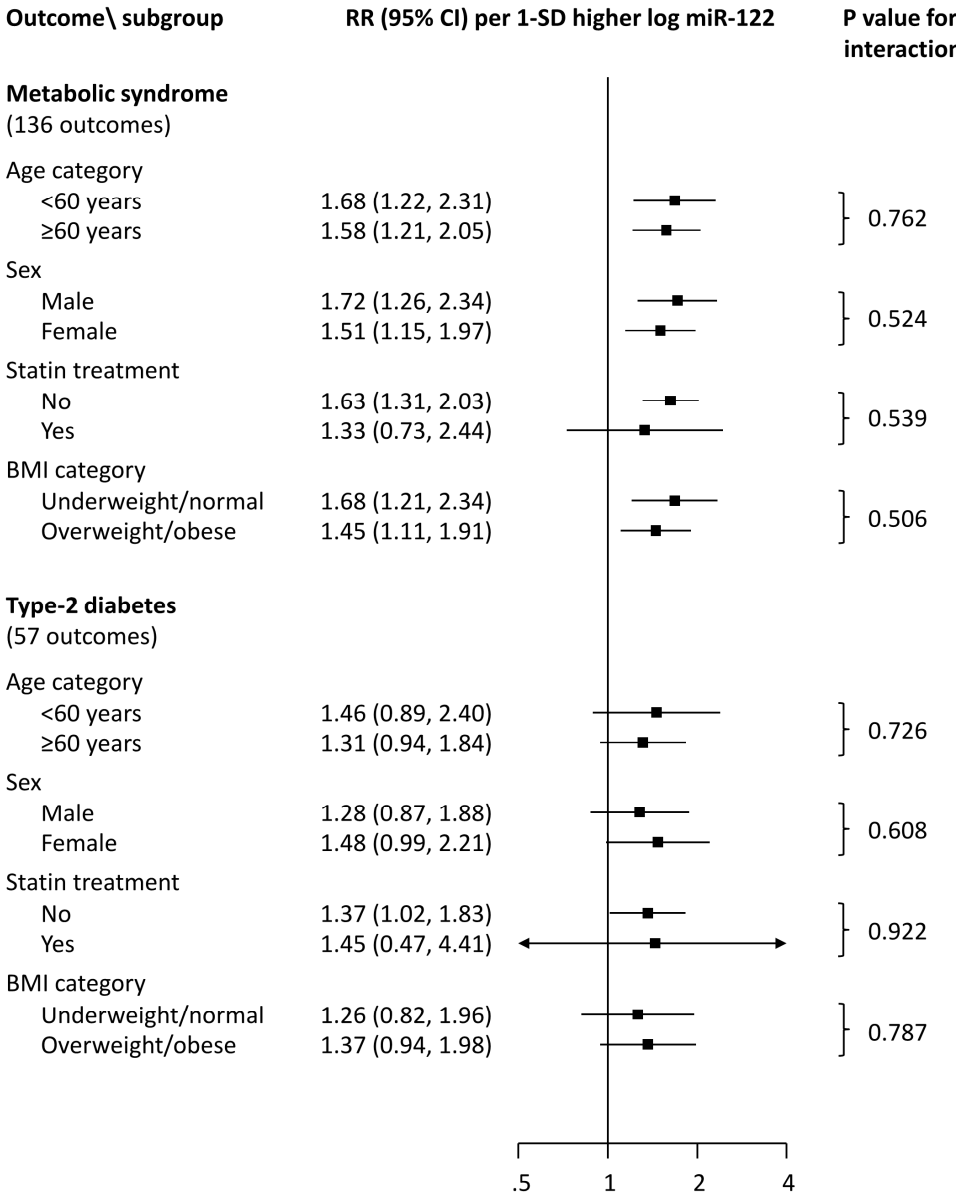

Risk ratios were adjusted for age, sex, socio-economic status, smoking, physical activity, and alcohol consumption.

Supplementary Figure 5 – Association of miR-122 with new-onset cardiovascular disease overall and across clinically relevant subgroups in the Bruneck Study.

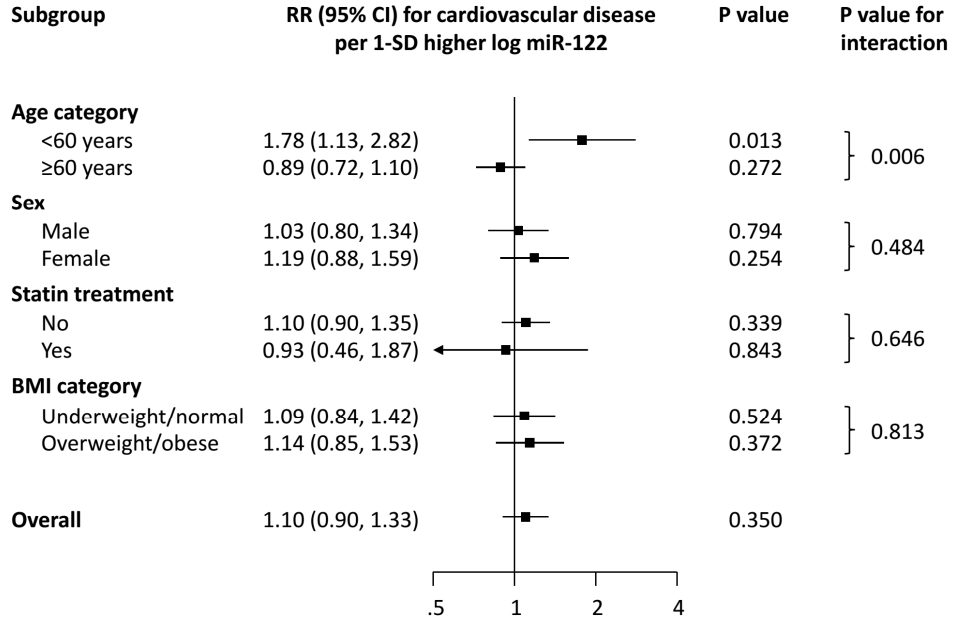

There were 108 new-onset events of cardiovascular disease. Risk ratios were adjusted for age, sex, socio-economic status, smoking, physical activity, and alcohol consumption.